

## Influence of misfit and bonding on the mode of growth in epitaxy

Jan H. van der Merwe and E. Bauer\*

*Department of Physics, University of Pretoria, Pretoria 0001, Republic of South Africa*

(Received 23 August 1988)

The relative stability of monolayer and double-layer epitaxial islands consisting of equal numbers of atoms is studied within the framework of the Frank–van der Merwe model as a function of island size, misfit, stiffness of the layer, and strength of film–substrate interaction. An exact solution of the governing equations has been obtained after linearization. The validity regimes of the results have been established. The main conclusion is that both registry strain energy and misfit energy considerably enhance the tendency to three-dimensional growth when the misfit becomes significant. At small misfit surface free energies are dominant. The predictions are compared with empirical data. Although some uncertainties still exist, the agreement with experiment is encouraging.

### I. INTRODUCTION

Epitaxial growth frequently starts with the formation of *monolayer* (ML) islands, even if the surface free energy  $\gamma_B$  of the film material *B* is larger than that ( $\gamma_A$ ) of the substrate, *A*. The thermodynamical equilibrium condition for ML formation,<sup>1</sup>

$$\Delta\gamma_{BA} \equiv \gamma_B + \gamma_i - \gamma_A \leq 0, \quad (1)$$

then requires that the interfacial free energy  $\gamma_i$  be negative, which means that there is only a small misfit and a strong *A–B* bond, and accordingly a strong tendency to alloy or compound formation. In the presence of misfit,  $\gamma_i$ , which contains the elastic strain energy in the ML and misfit energy of interfacial disregistry, increases with island size so that the ML condition may be violated beyond a critical island size. As a consequence, a transition from two-dimensional (2D) to three-dimensional (3D) growth may occur, provided it is not suppressed by kinetic limitations.

In an atomistic description using pairwise nearest-neighbor interaction energies  $E_{AA}$  and  $E_{BA}$  such a transition may even take place in the absence of misfit, simply on account of the dependence of the total energy  $E$  upon the number of *A* and *B* neighbors and its different dependence upon the total number  $N_0$  of atoms in a 2D and a 3D island.<sup>2</sup> The critical number  $N_c$  at which the 2D-3D transition occurs depends evidently on the relative magnitudes of  $E_{AA}$  and  $E_{BA}$ , as well as upon the island shapes. The problem of the 2D-3D transition arises also in the Stranski-Krastanov growth mode,<sup>1</sup> in which initially one to several 2D ML's are formed on top of which 3D crystals grow. It has been noted repeatedly that the 3D crystals not necessarily form by 3D nucleation but by a 2D-3D transition from 2D islands on top of the stable initial monolayer or multilayer.

The present paper addresses the question of the influence of misfit and bonding on the 2D-3D transition by calculating the relative stability of monolayer and multilayer islands with (approximately) equal total numbers of atoms  $N_0$  within the framework of the Frank–van

der Merwe model<sup>3</sup> and its “small-displacement” parabolic approximation, valid when there are no MD's and the maximum disregistry, occurring at the perimeter, are less than about a quarter of an atomic spacing. The theoretical predictions are then applied to specific epitaxial systems of current interest.

### II. THE MODEL

We wish to calculate the energy associated with the misfit between an epitaxial island and a substrate crystal for a monolayer (ML) island and a double-layer (DL) island—the thinnest 3D crystal—containing the same number  $N_0$  of atoms. Assuming that in both cases the atoms form quadratic arrays with a quadratic boundary, that there is an atom in the central position, and that the half-widths are  $M$  and  $N$  atomic spacings for the ML and the DL islands, respectively, we have

$$N_0 = (2M + 1)^2 = 2(2N + 1)^2. \quad (2)$$

Clearly the  $M$  as calculated for an integer  $N$  from this equation will not be an integer itself. This difficulty is overcome by treating specific cases and otherwise by approximating  $M$  and  $N$  as continuous (the continuity approximation)<sup>3,4</sup> variables.

We define the misfit in the conventional way as

$$f = (b - a) / a, \quad (3)$$

where  $a$  and  $b$  are the quadratic unit-cell dimensions in *A* and *B*, respectively. Because of the large disparity between the crystal thicknesses—the island is at most two atoms high—we neglect the strain in the substrate. Because this neglects the elastic relaxation of the substrate the calculated energy will be slightly in excess. Other simplifying approximations are that the crystals have simple cubic structure, satisfy isotropic elasticity, and are in parallel orientation.

Also the island atom-crystal interaction is represented by a truncated Fourier series<sup>3,4</sup>

$$V(x, y) = \frac{1}{2}W[2 - \cos(2\pi x/a) - \cos(2\pi y/a)], \quad (4)$$

where  $(x, y)$  defines the position of an interfacial island atom and the amplitude factor  $W$  may be related to the activation energy  $Q$  of surface migration and the desorption energy  $E_{\text{des}}$  (bond strength) approximately by<sup>4</sup>

$$W = Q = \kappa E_{\text{des}}, \quad 0.1 < \kappa < 0.33. \quad (5)$$

The proportionality factor  $\kappa$  depends strongly on bond type and surface crystallography. It is about  $\frac{1}{8}$  for W on W(110) (Ref. 5) and about  $\frac{1}{12}$  for Cu, Ag, and Au on W(110).<sup>6</sup> On the fcc (100) surface which also has two close packed directions  $\kappa$  is expected to have a similar value but on the rather open bcc (100) surface it should be larger.

We introduce integers  $(n, m)$  to enumerate interfacial island atoms and corresponding substrate potential troughs;  $n$  along  $x$  and  $m$  along  $y$ . It is convenient to describe atomic positions in terms of dimensionless displacements  $(\xi, \eta)$  defined by

$$\begin{aligned} x_{nm} &= a(n + \xi_{nm}), & y_{nm} &= a(m + \eta_{nm}), \\ \bar{x}_{nm} &= a(n + \bar{\xi}_{nm}), & \bar{y}_{nm} &= a(m + \bar{\eta}_{nm}), \end{aligned} \quad (6)$$

where  $(\bar{x}, \bar{y})$  and  $(\bar{\xi}, \bar{\eta})$  belong to the upper monolayer. Inserting (6) into (4) we obtain

$$V = \frac{1}{2} W [2 - \cos(2\pi\xi) - \cos(2\pi\eta)]. \quad (7)$$

In the analysis the need arises [see Eq. (17)] for replacing (7) by its small-displacement approximation, the parabolic potential<sup>7</sup>

$$V_p = W \pi^2 (\xi^2 + \eta^2). \quad (8)$$

The two expressions are compared in Fig. 1 for  $\eta=0$ . We adopt the criterion that  $V_p$  is an acceptable approximation for  $V$  provided

$$|\xi| \leq \frac{1}{4}, \quad |\eta| \leq \frac{1}{4}. \quad (9)$$

With this criterion the average discrepancy between  $V$  and  $V_p$  in the interval  $|\xi| \leq \frac{1}{4}$  is only about 13%, the maximum is about 23%. We shall see that the criterion (9) can easily be satisfied even for large islands if the misfit is small and the ratio of island atom-substrate to island atom-atom bonding large. In the foregoing we have tacitly assumed that the truncation (4) is a good approximation to the real potential. In some cases, presumably covalently bonded semiconductors the representation,<sup>8</sup> with an appropriate value of  $W$ , may even be closer to reality. However, the adoption of the parabolic potential for metals, like the adoption of a rigid substrate, will cause the calculated energies to be slightly in excess. Although the excess will be somewhat different in magnitude for the ML and DL islands it is believed to be so small that it will not effect the conclusions except in the case in which  $\Delta\gamma_{BA}$  is (very) near zero. In this case a small discrepancy

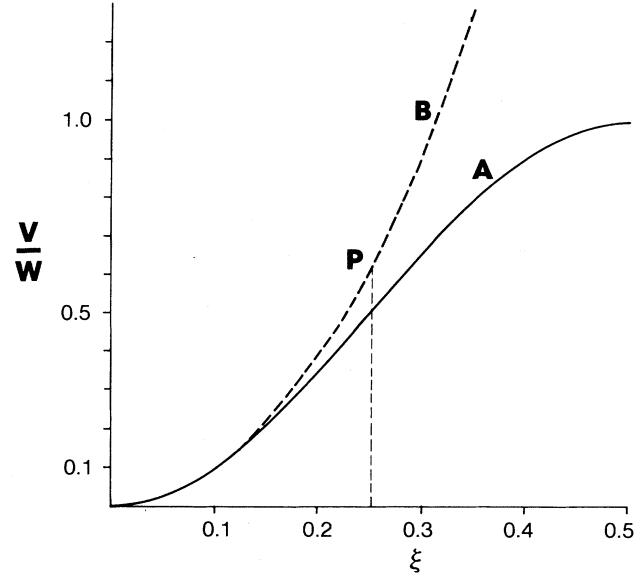


FIG. 1. Curves of the (island) atom-crystal interaction potential  $V$  in units of  $W$  vs atomic displacement  $\xi$ : curve  $A$  for the truncated Fourier series in Eq. (7) ( $\eta=0$ ) and curve  $B$  for the parabolic representation  $V_p$  in Eq. (8).  $P$  is acceptable limit.

may drastically effect the result.

We consider the DL island first. The ML case easily follows from the results. For the island atom-atom interaction we adopt the harmonic (elastic) approximation, applicable to small relative displacements and express the strain energy per atom in the form<sup>4</sup>

$$\begin{aligned} \varepsilon = \frac{\mu b^3}{1-\nu} [ & e_x^2 + e_y^2 + 2\nu e_x e_y + \frac{1}{2}(1-\nu)(e_{xz}^2 + e_{yz}^2) \\ & + \bar{e}_x^2 + \bar{e}_y^2 + 2\nu \bar{e}_x \bar{e}_y ], \end{aligned} \quad (10)$$

where the terms in  $e_{xz}$  and  $e_{yz}$  take account of the shear strains between the two ML's constituting the DL. For symmetry reasons shear strains in planes normal to the crystal surface are second-order small, being only a consequence of the Poisson effect. They have been deleted in Eq. (10). The strains are defined in terms of the displacements as<sup>4</sup>

$$\begin{aligned} e_x &= \delta(\xi_{n+1,m} - \xi_{nm} - f), & e_y &= \delta(\eta_{n,m+1} - \eta_{nm} - f), \\ e_{xz} &= \delta(\bar{\xi}_{nm} - \xi_{nm}), & e_{yz} &= \delta(\bar{\eta}_{nm} - \eta_{nm}), \\ \bar{e}_x &= \delta(\bar{\xi}_{n+1,m} - \bar{\xi}_{nm} - f), & \bar{e}_y &= \delta(\bar{\eta}_{n,m+1} - \bar{\eta}_{nm} - f), \end{aligned} \quad (11)$$

where  $\delta = a/b$ . The total energy  $E = \sum_{n,m} (V + \varepsilon)$  may now be written in the form

$$\begin{aligned}
E = \frac{1}{2} W \sum_{n,m} [2 - \cos(2\pi\xi_{nm}) - \cos(2\pi\eta_{nm})] + Wl^2 \sum_{n,m} [(\xi_{n+1,m} - \xi_{nm} - f)^2 + (\eta_{n,m+1} - \eta_{nm} - f)^2 \\
+ 2\nu(\xi_{n+1,m} - \xi_{nm} - f)(\eta_{n,m+1} - \eta_{nm} - f)] \\
+ Wl^2 \sum_{n,m} [(\bar{\xi}_{n+1,m} - \bar{\xi}_{nm} - f)^2 + (\bar{\eta}_{n,m+1} - \bar{\eta}_{nm} - f)^2 \\
+ 2\nu(\bar{\xi}_{n+1,m} - \bar{\xi}_{nm} - f)(\bar{\eta}_{n,m+1} - \bar{\eta}_{nm} - f)] \\
+ \frac{1}{2}(1-\nu)Wl^2 \sum_{n,m} [(\bar{\xi}_{nm} - \xi_{nm})^2 + (\bar{\eta}_{nm} - \eta_{nm})^2], \quad (12)
\end{aligned}$$

where

$$l^2 = \mu b a^2 / (1-\nu) W. \quad (13)$$

For the purpose of formulating the boundary conditions at the "vertical" boundary faces of the island we need expressions for the tensional forces acting on island planes made by vertical cuts parallel to the crystal axes:<sup>4</sup>

$$\begin{aligned}
T_x &= [2\mu b / (1-\nu)](e_x + \nu e_y), \\
\bar{T}_x &= [2\mu b / (1-\nu)](\bar{e}_x + \nu \bar{e}_y) \quad (14)
\end{aligned}$$

with similar expressions for  $T_y$  and  $\bar{T}_y$ . At the free boundaries (edges at  $n=N, m=N$ ) the relations

$$0 = T_x = \bar{T}_x = T_y = \bar{T}_y \quad (15)$$

must be satisfied.

### III. GOVERNING EQUATIONS AND THEIR SOLUTIONS: DL ISLAND

The equations governing the atomic positions in the DL island are determined by the minimum-energy equilibrium principle, i.e., that in the equilibrium configuration  $0 = \partial E / \partial \xi_{nm} = \dots$ , etc. We obtain from relation (12)

$$\begin{aligned}
\xi_{n+1,m} - 2\xi_{nm} + \xi_{n-1,m} + \nu(\eta_{n+1,m} - \eta_{nm} + \eta_{n-1,m}) \\
+ \frac{1}{2}(1-\nu)(\bar{\xi}_{nm} - \xi_{nm}) = (\pi/2l^2)\sin(2\pi\xi_{nm}), \\
\bar{\xi}_{n+1,m} - 2\bar{\xi}_{nm} - \bar{\xi}_{n-1,m} + \nu(\bar{\eta}_{n+1,m} - \bar{\eta}_{nm} + \bar{\eta}_{n-1,m}) \\
- \frac{1}{2}(1-\nu)(\bar{\xi}_{nm} - \xi_{nm}) = 0 \quad (16)
\end{aligned}$$

and two similar equations for  $\partial E / \partial \eta_{nm} = \partial E / \partial \bar{\eta}_{nm} = 0$ .

These are nonlinear coupled second-order difference equations. They can only be solved if two additional simplifying approximations are made: first that  $\xi$  and  $\eta$  are small enough so that the parabolic approximation (8) is acceptable, and second that the variations of  $\xi$  and  $\eta$  (from atom to atom) are so slow that we may use the continuum<sup>3,4</sup> approximation, e.g.,  $\xi_{nm} \approx \xi(n, m)$  and  $\xi_{n+1,m} - 2\xi_{nm} + \xi_{n-1,m} \approx \partial^2 \xi / \partial n^2$ . The governing equations (16) accordingly linearize

$$\begin{aligned}
0 = \frac{\pi^2}{l^2} \xi - \frac{\partial^2 \xi}{\partial n^2} - \nu \frac{\partial^2 \eta}{\partial n^2} - \frac{1-\nu}{2} (\bar{\xi} - \xi), \\
0 = -\frac{\partial^2 \xi}{\partial n^2} - \nu \frac{\partial^2 \bar{\eta}}{\partial n^2} + \frac{1-\nu}{2} (\bar{\xi} - \xi). \quad (17)
\end{aligned}$$

For symmetry reasons we may have solutions of the kind

$$\begin{aligned}
\xi = \xi(n), \quad \bar{\xi} = \bar{\xi}(n), \\
\eta = \eta(m), \quad \bar{\eta} = \bar{\eta}(m), \quad (18)
\end{aligned}$$

by which the governing equations separate in pairs:

$$\frac{d^2 \xi}{dn^2} = \beta^2 \xi - \alpha^2 (\bar{\xi} - \xi), \quad \frac{d^2 \bar{\xi}}{dn^2} = \alpha^2 (\bar{\xi} - \xi), \quad (19a)$$

$$\frac{d^2 \eta}{dm^2} = \beta^2 \eta - \alpha^2 (\bar{\eta} - \eta), \quad \frac{d^2 \bar{\eta}}{dm^2} = \alpha^2 (\bar{\eta} - \eta), \quad (19b)$$

and we have used the abbreviated notation

$$\beta = \pi/l, \quad \alpha^2 = (1-\nu)/2. \quad (20)$$

The appropriate solutions of Eqs. (19) must be antisymmetric, i.e.,

$$\xi/f = A_1 \sinh(\gamma_1 n) + A_2 \sinh(\gamma_2 n), \quad (21a)$$

$$\bar{\xi}/f = B_1 \sinh(\gamma_1 n) + B_2 \sinh(\gamma_2 n),$$

$$\eta/f = A_1 \sinh(\gamma_1 m) + A_2 \sinh(\gamma_2 m), \quad (21b)$$

$$\bar{\eta}/f = B_1 \sinh(\gamma_1 m) + B_2 \sinh(\gamma_2 m).$$

It follows by substitution of (21a) into (19a) that

$$B_{1,2} = p_{1,2} A_{1,2}, \quad p_{1,2} = (\alpha^2 + \beta^2 - \gamma_{1,2}^2) / \alpha^2, \quad (22a)$$

$$\gamma_{1,2} = Q_{1,2} \pm Q_2, \quad Q_{1,2} = [(\beta^2/2 + \alpha^2 \pm \alpha\beta)/2]^{1/2}. \quad (22b)$$

The integration constants  $A_1$  and  $A_2$  are determined by the boundary conditions (15).

In the continuum approximation the relations (11) become

$$\begin{aligned}
e_x / \delta = d\xi/dn - f = f\gamma_1 A_1 \cosh(\gamma_1 n) \\
+ f\gamma_2 A_2 \cosh(\gamma_2 n) - f, \quad (23a)
\end{aligned}$$

$$\begin{aligned}
\bar{e}_x / \delta = d\bar{\xi}/dn - f = fp_1 \gamma_1 A_1 \cosh(\gamma_1 n) \\
+ fp_2 \gamma_2 A_2 \cosh(\gamma_2 n) - f, \quad (23b)
\end{aligned}$$

$$\begin{aligned}
e_y / \delta = d\eta/dm - f = f\gamma_1 A_1 \cosh(\gamma_1 m) \\
+ f\gamma_2 A_2 \cosh(\gamma_2 m) - f, \quad (23c)
\end{aligned}$$

$$\begin{aligned}
\bar{e}_y / \delta = d\bar{\eta}/dm - f = fp_1 \gamma_1 A_1 \cosh(\gamma_1 m) \\
+ fp_2 \gamma_2 A_2 \cosh(\gamma_2 m) - f. \quad (23d)
\end{aligned}$$

Also from Eqs. (14) and (15) the boundary conditions at  $n=N$  takes the form

$$0 = T_x = [2\mu b / (1 - \nu)] [e_x(N) + \nu e_y(m)]. \quad (24a)$$

This equation cannot be identically satisfied because of the dependence of  $e_y$  on  $m$ . The reason for this dependence is that the Poisson contraction induces a slight curvature into the free boundary which cannot be described by the simple solutions in Eq. (18).<sup>8</sup> Since it is a small effect we can overcome the difficulty (approximately) by ignoring the Poisson effect in Eq. (24a) setting  $\nu=0$ , or overestimate the effect by noting that the effect will be most notable in the middle ( $m=0$ ) of the boundary at  $n=N$  setting  $m=0$  and  $\nu=\nu'$ . We adopt the second course because it includes the first one as a limiting case if we replace Eq. (24a) and its equivalent for the upper ML, respectively, by

$$e_x(N) + \nu' e_y(0) = 0, \quad \bar{e}_x(N) + \nu' \bar{e}_y(0) = 0, \quad 0 \leq \nu' \leq \nu. \quad (24b)$$

In these relations,  $\nu'$  is an adjustable parameter which we may choose appropriately. Furthermore since symmetry requires  $e_y(N) = e_x(N)$ ,  $e_y(0) = e_x(0)$ , these equations also define boundary conditions at  $m=N$ . If we substitute

$$\begin{aligned} \frac{E}{4Wl^2} = \int_0^N dn \int_0^N dm \left[ \beta^2 \xi^2 + \alpha^2 (\bar{\xi} - \xi)^2 + \left( \frac{d\xi}{dn} - f \right)^2 + \left( \frac{d\bar{\xi}}{dn} - f \right)^2 + \beta^2 \eta^2 + \alpha^2 (\bar{\eta} - \eta)^2 + \left( \frac{d\eta}{dm} - f \right)^2 \right. \\ \left. + \left( \frac{d\bar{\eta}}{dm} - f \right)^2 + 2\nu \left[ \left( \frac{d\xi}{dn} - f \right) \left( \frac{d\eta}{dm} - f \right) + \left( \frac{d\bar{\xi}}{dn} - f \right) \left( \frac{d\bar{\eta}}{dm} - f \right) \right] \right]. \quad (27) \end{aligned}$$

If we substitute from Eqs. (21)–(25), it follows after a somewhat tedious but straightforward calculation, that we may express the mean energy per DL island atom in the form

$$\epsilon^{\text{DL}} \equiv \frac{E^{\text{DL}}}{2Wl^2 f^2 (2N+1)^2} \equiv \left[ \frac{2N}{2N+1} \right]^2 F^{\text{DL}}, \quad (28a)$$

$$\begin{aligned} F^{\text{DL}} = \left\{ \frac{1}{PN} \left[ (P-1)(q_1-2) \frac{q_1 t_1}{\gamma_1} + (P+1)(q_2-2) \frac{q_2 t_2}{\gamma_2} \right] + 2(1+\nu) - \frac{2\nu}{PN} \left[ (P-1) \frac{q_1 t_1}{\gamma_1} + (P+1) \frac{q_2 t_2}{\gamma_2} \right] \right. \\ \left. + \frac{\nu}{PN^2} \left[ (P-1) \left[ \frac{q_1 t_1}{\gamma_1} \right]^2 + (P+1) \left[ \frac{q_2 t_2}{\gamma_2} \right]^2 \right] \right\}, \quad (28b) \end{aligned}$$

$$P = (1 + \beta^4 / 4\alpha^4)^{1/2}, \quad t_{1,2} = \tanh(\gamma_{1,2} N). \quad (28c)$$

For the extreme case of perfect registry, defined in Eq. (26), we obtain from (27) and (28)

$$\epsilon_{\text{reg}}^{\text{DL}} = \left[ \frac{2N}{2N+1} \right]^2 F_{\text{reg}}^{\text{DL}} = 2(1+\nu) \left[ \frac{2N}{2N+1} \right]^2. \quad (29)$$

#### V. MONOLAYER ISLAND

The corresponding relations for the ML island may be simply obtained from the foregoing. Since the second layer is absent in the ML case the shear, defined in Eq. (11), and the terms containing  $\bar{e}$ , are absent from Eq. (10). Equations (19) and (27) accordingly reduce, respectively, to

$$\frac{d^2 \xi}{dn^2} - \beta^2 \xi = 0, \quad \frac{d^2 \eta}{dm^2} - \beta^2 \eta = 0 \quad (30)$$

from Eqs. (22) and (23) into (24b) we may solve for the constants, obtaining

$$A_1 = \frac{q_1(1-p_2)}{\gamma_1(p_1-p_2)\cosh(\gamma_1 N)}, \quad (25a)$$

$$A_2 = \frac{q_2(1-p_1)}{\gamma_2(p_2-p_1)\cosh(\gamma_2 N)},$$

$$q_{1,2} = (1+\nu') / [1 + \nu' \text{sech}(\gamma_{1,2} N)]. \quad (25b)$$

Of some interest is the limiting case in which the entire island is homogeneously deformed into *perfect registry* with the substrate so that

$$\xi = \bar{\xi} = \eta = \bar{\eta} \equiv 0. \quad (26)$$

#### IV. ENERGY: DL ISLAND

The energy induced by the competing forces may be calculated from the relation in Eq. (12) using the continuum approximation that has led to Eqs. (17), the parabolic approximation (8), and the relations (18):

and

$$\begin{aligned} \frac{E^{\text{ML}}}{4Wl^2} = \int_0^M dn \int_0^M dm \left[ \beta^2 (\xi^2 + \eta^2) \right. \\ \left. + \left( \frac{d\xi}{dn} - f \right)^2 + \left( \frac{d\eta}{dm} - f \right)^2 \right. \\ \left. + 2\nu \left[ \left( \frac{d\xi}{dn} - f \right) \left( \frac{d\eta}{dm} - f \right) \right] \right]. \quad (31) \end{aligned}$$

The appropriate solutions of Eqs. (30) are the antisymmetric ones

$$\xi(n) = f A \sinh(\beta n), \quad \eta(m) = f A \sinh(\beta m), \quad (32)$$

so that

$$\begin{aligned} \frac{d\xi}{dn} - f &= f\beta A \cosh(\beta n) - f, \\ \frac{d\eta}{dm} - f &= f\beta A \cosh(\beta m) - f. \end{aligned} \quad (33)$$

The integration constant follows from the boundary condition (24) as

$$A = (1 + \nu') / \beta [\cosh(\beta M) + \nu']. \quad (34)$$

It is easily shown, using (32)–(34), that if the acceptability criterion (9) is met for a DL island, it will also be met for a ML island whose half-width  $M$  is defined by (2).

If we now substitute from (32)–(34) into (31) we obtain for the mean energy per ML island atom [in analogy to Eq. (28)] the result

$$\begin{aligned} \epsilon^{\text{ML}} &\equiv \frac{E^{\text{ML}}}{2Wl^2 f^2 (2N+1)^2} \equiv \left[ \frac{2M}{2N+1} \right]^2 F^{\text{ML}}(\beta, M), \\ F^{\text{ML}}(\beta, M) &= \frac{A \sinh(\beta M)}{M} \\ &\times \left[ \frac{A}{M[\beta M \cosh(\beta M) + \nu \sinh(\beta M)]} \right. \\ &\quad \left. - 2(1 + \nu) \right] + 1 + \nu. \end{aligned} \quad (35a)$$

Applying relations analogous to those that have led to Eqs. (29), we obtain for the ML island

$$\epsilon_{\text{reg}}^{\text{ML}} = \frac{E_{\text{reg}}^{\text{ML}}}{2Wl^2 f^2 (2N+1)^2} = (1 + \nu) \left[ \frac{2M}{2N+1} \right]^2. \quad (35b)$$

It has, in the past, often been assumed in semiquantitative considerations that a double layer comprising two monatomic layers can be described by the formalism of a monolayer, replacing  $\mu$  by  $2\mu$ —alternatively  $b$  in Eq. (13) by  $2b$ . This approach essentially neglects the strain gradient normal to the film plane and introduces, in analogy to Eqs. (13) and (20), the relations

$$l_2^2 = 2l^2, \quad \beta_2^2 = \pi^2 / l_2^2 = \beta^2 / 2. \quad (36)$$

The present calculations allow us to estimate the error involved in this approach. The energy of such an episystem may be calculated from the integral in Eq. (31), integrating up to  $N$  rather than  $M$ , yielding instead of (35) the result

$$\epsilon_1^{\text{DL}} = \frac{E_1^{\text{DL}}}{2Wl_2^2 f^2 (2N+1)^2} = \left[ \frac{2N}{2N+1} \right]^2 F^{\text{ML}}(\beta_2, N). \quad (37a)$$

The equivalent of Eq. (35b) likewise follows as

$$\epsilon_{1,\text{reg}}^{\text{DL}} = \frac{E_{1,\text{reg}}^{\text{DL}}}{2Wl_2^2 f^2 (2N+1)^2} = (1 + \nu) \left[ \frac{2N}{2N+1} \right]^2. \quad (37b)$$

## VI. DISCUSSION

We wish to compare the energetics of monolayer (ML) and double-layer (DL) islands, consisting of the same

numbers of atoms [see Eq. (2)], in order to establish the influence of interfacial misfit and bonding, and hence of the resulting misfit and misfit strain energy, on the growth mode. The ML and DL islands must consist of integer numbers of atoms,  $M$  and  $N$ . For any integer  $N$  the solution  $M'$  for  $M$  from (2) is irrational though. In the range of small  $N$ —the present interest—relation (2) defines integer pairs  $(N, M) = (2, 3)$  and  $(7, 10)$  for which  $M = 3$  and  $10$  differ from  $M'$  by only about 1%. These two cases will accordingly receive special consideration. In order to estimate the values of  $M$  and  $N$  at which the 2D to 3D transition may occur, it will also be useful to treat  $M$  and  $N$  as continuous variables.

The foregoing analysis suggests that the natural vehicle for introducing atomic bonding is through the parameter  $l$  in Eq. (13); thus

$$l^2 = \frac{\pi^2}{\beta^2} = \frac{\mu a^2 b}{(1 - \nu)W}, \quad (38)$$

for an overlayer  $B$  on a substrate  $A$ ;  $A$  taken as reference. We may similarly write down  $l_0^2$  for  $A$  on  $A$  and define a bond ratio

$$\omega = \frac{l_0^2}{l^2} = \frac{\beta^2}{\beta_0^2} = \frac{\mu_0(1 - \nu)Wa}{\mu(1 - \nu_0)W_0b} = \frac{\omega_0}{1 + f}, \quad (39a)$$

$$\omega_0 = \frac{\mu_0(1 - \nu)W}{\mu(1 - \nu_0)W_0}. \quad (39b)$$

The misfit  $f$  is defined in Eq. (3). Thus  $\omega_0$ , in (39b), is the true bond ratio depending on  $\mu/\mu_0$  and  $W/W_0$  but not on  $f$ .

Also, for  $B$  on  $A$  it is seen from (28a)–(29) and (35)–(37) that the energy is proportional to

$$\begin{aligned} Wl^2 &= W_0 l_0^2 \frac{\mu(1 - \nu_0)(1 + f)}{\mu_0(1 - \nu)} = W_0 l_0^2 \frac{W}{\omega W_0} \\ &= \frac{\mu_0 a^3}{1 - \nu_0} \frac{W}{\omega W_0}. \end{aligned} \quad (40)$$

Previously,<sup>9</sup>  $l_0$  has been shown to be about 6. It is convenient to take  $l_0 = 2\pi$ , and hence from (20),  $\beta_0 = 0.5$ . It accordingly follows from (39) that

$$\beta^2 = \beta_0^2 \omega = 0.25\omega. \quad (41)$$

Also, when a numerical value is needed for the ratio  $(1 - \nu_0)/(1 - \nu)$  we shall make the conventional assumption that  $\nu = \nu_0 = \frac{1}{3}$ .

It is of interest to establish the validity regimes of the acceptability criterion (9), i.e., to find the values of  $f$  and  $\omega$  for which the condition  $\xi(f, \omega; N) \leq \frac{1}{4}$  is satisfied. In  $(f, \omega)$  space the boundary line for given  $N$  is defined by the relation

$$\xi(f, \omega; N) = \frac{1}{4}. \quad (42)$$

With Eq. (21) this gives the implicit equation

$$\begin{aligned} f(\omega; \nu', N) &= 1/4 [A_1 \sinh(\gamma_1 N) + A_2 \sinh(\gamma_2 N)] \\ &\equiv 1/4 \phi(\omega_0, \nu', f; N), \end{aligned} \quad (43)$$

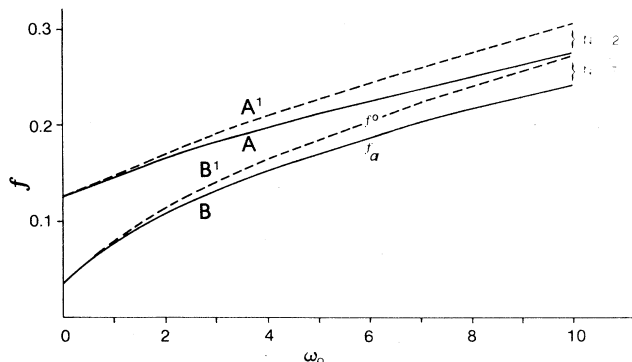


FIG. 2. Maximum misfit  $f = f_a$  for which the potential approximation (8) is acceptable as a function of the parameter  $\omega_0$  [Eq. (39b)]. The curves are the solutions  $(f, \omega_0)$  of Eq. (43) for  $\nu = 0.2$  [Eq. (44)] and  $\nu = \frac{1}{3}$ : curve  $A$  for  $N=2$  and curve  $B$  for  $N=7$ . At  $\omega_0=0$ ,  $f=1/4N$ . Curves  $A'$  and  $B'$  represent the corresponding zeroth-order solutions  $f^0$ .

the quantities  $\gamma_{1,2}, \nu', A_{1,2}$ , and  $\omega_0$  being defined by Eqs. (22), (24b), (25), and (39), respectively. The acceptable values of  $f$  are those below the curve of  $f_a \equiv f(\omega_0; \nu', N)$ , for fixed values of  $\nu'$  and  $N$ ,  $f_a$  being the exact solution of Eq. (43).

The implicit equation (43) is dealt with iteratively,  $f^0 = 1/4\phi(\omega_0, \nu', 0, N)$ ,  $f^1 = 1/4\phi(\omega_0, \nu', f^0, N)$ , and  $f^\infty \equiv f_a$  being the zeroth-order, first-order, and final solutions, respectively. We have carried out calculations covering the intervals  $0 \leq \omega_0 \leq 10$  and  $0 \leq \nu' \leq \nu$  for  $N=2$  and 7. The most notable result is that the convergence is rapid; while  $f^0$  differs from  $f_a$  by about 20%,  $f^1$  is within 2% of  $f_a$ . The dependence of  $f_a$  on  $\omega_0$  and  $\nu'$  are

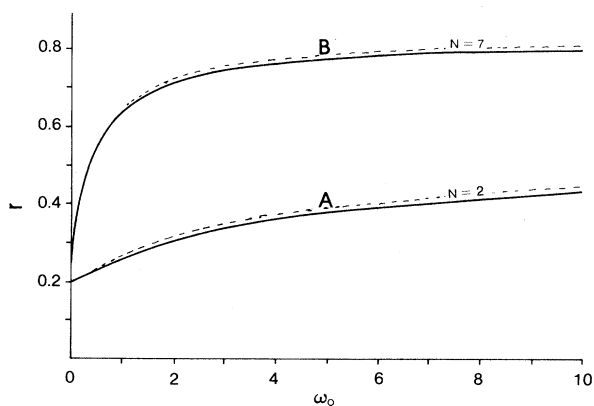


FIG. 3. Ratio  $r = \epsilon^{\text{DL}}/\epsilon^{\text{ML}}$  [Eq. (46)] of energy per atom in double (DL) and monolayer (ML) islands with (approximately) equal numbers of atoms [Eq. (2)] as a function of the parameter  $\omega_0$  [Eq. (39b)]: curves  $A$  and  $B$  for  $N=2$  and  $N=7$ , respectively, and misfit  $f$  as defined by Eq. (43) and displayed by curves  $A$  and  $B$  in Fig. 2. The dotted curves are the corresponding ones, but for  $f=0.05$ . The curves for  $f=0.1$  lie between each pair consisting of dotted and solid lines.

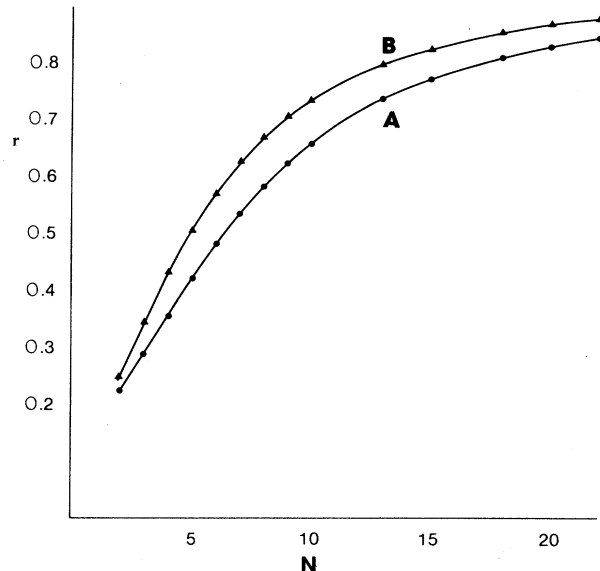


FIG. 4. Curves of the energy ratio  $r = \epsilon^{\text{DL}}/\epsilon^{\text{ML}}$  [Eq. (46)] vs DL island size  $N$  ( $N$  and  $M$  treated as continuous variables) for bonding parameter [defined in Eq. (39b)]  $\omega_0=0.5$  (curve  $A$ ) and  $\omega_0=1.0$  (curve  $B$ ).

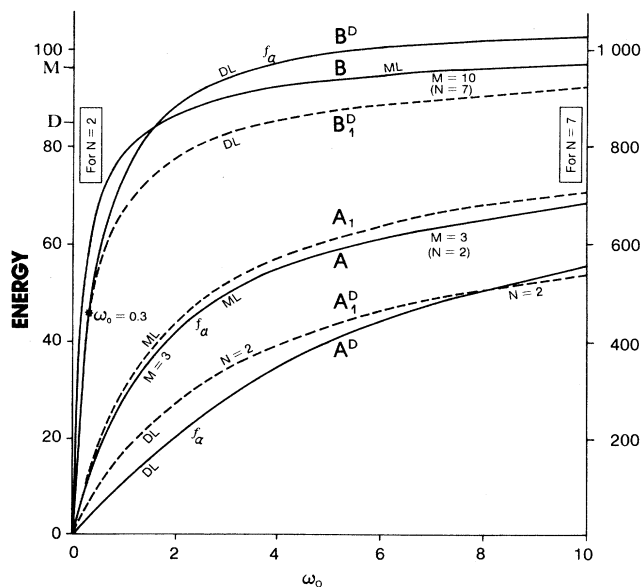


FIG. 5. Curves displaying the variation of ML- and DL-island total energies, respectively,  $E^{\text{ML}}/E_0^{\text{ML}} = 2(2M)^2 F^{\text{ML}}(\beta, M)$  [Eqs. (47)] and  $E^{\text{DL}}/E_0^{\text{DL}} = 4(2N)^2 F^{\text{ML}}(\beta, N)$  [Eq. (37a)] vs  $\omega_0$  in units of  $E_0^{\text{ML}} = \mu a^3(1+f)f^2/(1-\nu)$ , where the two ML's constituting the DL island are constrained to undergo the same deformation: (a)  $A, A_1$  for ML's ( $M=3$ );  $f=f_a$  from Eq. (43) and  $f=0.05$ , (b)  $B$  for a ML's ( $M=10$ );  $f=f_a$ , (c)  $A^D$  and  $A_1^D$  for DL's ( $N=2$ );  $f=f_a$  and  $f=0.05$ , and (d)  $B^D$  and  $B_1^D$  for DL's ( $N=7$ );  $f=f_a$  and  $f=0.05$ . The values designated  $D$  and  $M$  represent, respectively,  $E_{1,\text{reg}}^{\text{DL}}/E_0^{\text{ML}}$  and  $E_{\text{reg}}^{\text{ML}}/E_0^{\text{ML}}$ .

significant;  $f_a$  increases monotonically from  $1/4N$  (at  $\omega_0=0$ ) as  $\omega_0$  increases, but decreases monotonically as  $\nu'$  increases from  $\nu'=0$  to  $\nu'=\frac{1}{3}$ . At  $\omega_0=10$  (a rather high value)  $f_a$  decreases from about 0.5 to 0.4, i.e., by about 25%, when  $\nu'$  increases from 0 to  $\frac{1}{3}$ . Clearly the truth is somewhere between  $\nu'=0$  and  $\nu'=\frac{1}{3}$ , possibly closer to  $\nu'=\frac{1}{3}$ . We adopt a value of

$$\nu'=0.2 \quad (44)$$

knowing that the effect on relative values of calculated quantities will be small. The dependences of  $f^0$  and  $f_a$  on  $\omega_0$  for  $N=2$  and 7 are displayed in Fig. 2.

In order to assess the contribution of misfit and bonding to the energetic preference for 2D or 3D growth we need to know: (a) the relative magnitudes of the energies per atom  $\epsilon^{\text{DL}}$  and  $\epsilon^{\text{ML}}$  so that we can establish the direction of the related driving force, and (b) the magnitudes of these energies as compared to free-surface energies. We may thus assess their ability of swaying the growth towards one mode or the other.

We begin by comparing the energies in the limiting case in which the islands are homogeneously strained into registry as defined by Eq. (26). From Eqs. (2), (29), and (35) it is seen that

$$r_{\text{reg}} \equiv \epsilon_{\text{reg}}^{\text{DL}} / \epsilon_{\text{reg}}^{\text{ML}} = 2(N/M)^2. \quad (45)$$

For the specific cases  $(N, M) = (2, 3)$  and  $(7, 10)$ , representing respectively "small" and "large" islands, it follows that  $r_{\text{reg}} \lesssim 1$ .

We may write for the general case

$$\begin{aligned} r(N, \omega_0, f, \nu', \nu) &= \frac{E^{\text{DL}}}{E^{\text{ML}}} \\ &= \frac{\epsilon^{\text{DL}}}{\epsilon^{\text{ML}}} = \left[ \frac{N}{M} \right]^2 \frac{F^{\text{DL}}(N, \omega_0, f, \nu', \nu)}{F^{\text{ML}}(M, \omega_0, f, \nu', \nu)}, \end{aligned} \quad (46)$$

using Eqs. (2), (22), (25), (28), and (35a). It is useful to investigate the dependence of  $r$  on  $\omega_0$ : (a) for  $f$  values satisfying Eq. (43), i.e., for the maximum misfit for which the potential approximation (8) is acceptable, and (b) for fixed  $f=0.1$  and  $f=0.05$ , bearing in mind that the results are meaningful for  $f=0.1$  only when  $\omega_0$  is greater than the value defined by Eq. (43). The results are displayed in Fig. 3 for small ( $N=2$ ) and large ( $N=7$ ) islands. The

curves for  $f=0.1$  lie between the members of each pair, consisting of a dotted and solid line, and are not shown.

In Fig. 4 we compare the variation of the ratio  $r$  with  $N$  for  $\omega_0=0.5$  (curve *A*) and 1.0 (curve *B*). Apart from the fact that the dependence illustrated in the curve is interesting in itself, it also demonstrates the expectation that a crossover between curves *A* and *B* as well as a crossover between the mechanical energies of DL and ML islands ( $r$  increasing from below, to above unity) is not possible.

Having determined the relative values of  $E^{\text{DL}}$  and  $E^{\text{ML}}$  we shall know both if we know one of them. We pick the one with the simpler formulation, namely,  $E^{\text{ML}}$  in Eq. (35a). One remaining difficulty is that both are proportional to  $Wl^2$ , which does not simply depend on  $\omega$ , but rather on parameters appearing separately in  $\omega$ , as may be seen in Eq. (40). And, of course, if we wish to analyze the dependence of  $E^{\text{ML}}$  on  $\omega$  we are limited to the acceptability domain whose upper bound is defined by Eq. (43). We consider the acceptable regimes of  $\omega$  for  $f=0.10$  and 0.05, and write

$$E^{\text{ML}} = 2(2M)^2 F^{\text{ML}} E_0^{\text{ML}}, \quad (47a)$$

$$E_0^{\text{ML}} = \frac{W_0 l_0^2 \mu (1-\nu_0) (1+f) f^2}{\mu_0 (1-\nu)} = \frac{\mu a^3 (1+f) f^2}{1-\nu} = Wl^2 f^2, \quad (47b)$$

using Eqs. (35a), (38), and (40). Curves of  $E^{\text{ML}}$  and  $E^{\text{DL}}$  versus  $\omega_0$  in units of  $E_0^{\text{ML}}$  are displayed in Fig. 5. The limiting value  $E_{\text{reg}}^{\text{ML}}$  in Eq. (35b) and  $E_{1,\text{reg}}^{\text{DL}}$  in Eq. (37b), are also indicated in Fig. 5 as *M* and *D*, respectively. A numerical value of  $E^{\text{ML}}$  for given  $W_0 l_0^2$  in Eq. (41a), given  $\omega_0$  in Eq. (39b), and given  $f$  is obtained from the figure by scaling with the ratio  $\mu(1-\nu_0)/\mu_0(1-\nu)$  occurring in both  $E_0^{\text{ML}}$  and  $\omega_0$ .

We wish to compare the energy contributions of purely electronic nature and the contributions  $E^{\text{ML}}$  and  $E^{\text{DL}}$  due to disregistry and strain. With the conventional assumptions that, particularly (i) a ML is macroscopic, (ii) the surface free energy is isotropic, and (iii) the structure is simple cubic, the growth mode criterion [see Eq. (1)] for *B* on *A*—excluding the contributions of the side faces, disregistry and strain—is<sup>1</sup>

$$(2M+1)^2 a^2 (\gamma_B + \gamma_{BA}^0 - \gamma_A) \equiv (2M+1)^2 a^2 \Delta \gamma_{BA}^0 \begin{cases} < 0 & \text{for FM} \\ > 0 & \text{for VW} \end{cases}, \quad (48)$$

where  $\gamma_{BA}^0$  is the electronic contribution to the interfacial free energy in the absence of misfit and  $(2M+1)^2$  is the number of atoms  $N_0$  in Eq. (2). VW refers to the Volmer-Weber and FM to the Frank-van der Merwe mechanism for the growth of thin crystalline films near equilibrium. If the energies of the side faces, as well as the energy of disregistry and strain when misfit exists are included, the criterion generalizes to

$$\begin{aligned} (2M+1)^2 a^2 \Delta \gamma_{BA}^0 - (2M+1)^2 a^2 \gamma_A + E^{\text{ML}} &\begin{cases} < (2N+1)^2 a^2 \Delta \gamma_{BA}^0 - (2N+1)^2 a^2 \gamma_B + E^{\text{DL}} & \text{for FM} \\ > (2N+1)^2 a^2 \Delta \gamma_{BA}^0 - (2N+1)^2 a^2 \gamma_B + E^{\text{DL}} & \text{for VW} \end{cases}, \\ \Delta \gamma_{BA}^0 - \frac{8(\sqrt{2}-1)}{2M+1} \gamma_B + \frac{2(E^{\text{ML}} - E^{\text{DL}})}{(2M+1)^2 a^2} &\begin{cases} < 0 & \text{for FM} \\ > 0 & \text{for VW} \end{cases}. \end{aligned} \quad (49)$$

Here we have made use of Eq. (2). The second term on the right comes from taking the side surfaces of the DL and ML islands into account. It follows from Eqs. (35a), (40), and (46) that

$$E^{\text{ML}} - E^{\text{DL}} = (2M)^2 2W_0 l_0^2 f^2 (W/W_0 \omega) (1-r) F^{\text{ML}}(\beta, M). \quad (50)$$

Combining Eqs. (50), (39), and (40b) the growth mode criterion in Eq. (49) becomes

$$\Delta\gamma_{BA}^0 - \frac{8(\sqrt{2}-1)}{2M+1} \gamma_B + 4a \left[ \frac{2M}{2M+1} \right]^2 \frac{\mu}{1-\nu} f^2 (1+f)(1-r) F^{\text{ML}} \begin{cases} < 0 & \text{for FM} \\ > 0 & \text{for VW}; r < 1. \end{cases} \quad (51)$$

The ratio  $r$  is given by Eq. (46) and illustrated in Figs. 3 and 4, whereas  $F^{\text{ML}}$  is given by Eq. (35a) and illustrated in Fig. 5. Since  $r$  and  $F^{\text{ML}}$  depend in a complex manner upon  $M$ ,  $\mu$ ,  $\nu$ ,  $W$ ,  $\mu_0$ ,  $\nu_0$ ,  $W_0$ , and  $f$ , this relation is difficult to analyze. It does, however, clearly show that misfit favors VW growth as do positive values of  $\Delta\gamma_{AB}^0$ , whereas negative values of  $\Delta\gamma_{AB}^0$  and the contribution of the lateral boundaries of the islands favor FM growth. The excess of one or the other implies the existence of a driving force towards the relevant growth mode. The contribution from the side faces is seen to decrease with island size.

## VII. COMPARISON WITH EXPERIMENT

Reliable predictions on the basis of Eq. (51) are not only hard to make because of the difficulty of evaluating the second term in it, but also because of the lack of data for  $\gamma_{BA}^0$  in  $\Delta\gamma_{BA}^0$ . Nevertheless a few examples of current interest in which  $\gamma_B > \gamma_A$  will be discussed briefly. Such systems are fcc, Fe, fcc Co and Ni on Cu(100), and bcc Fe and Cr on Ag(100) and Au(100). The interatomic distances  $d$  (defining the misfit) and the surface energies  $\gamma$  as taken from Ref. 10, are listed in Table I. Estimates of  $\gamma_{BA}^0$  (in  $\text{J m}^{-2}$ ) are Co/Cu, +0.20;<sup>11</sup> Ni/Cu+0.02;<sup>11</sup> Fe/Cu, +0.40;<sup>12</sup> Fe/Ag, +0.62;<sup>12</sup> Fe/Au, +0.19;<sup>12</sup> and Cr/Ag, +0.57.<sup>13</sup>

For fcc Fe, fcc Co, and Ni on {100} Cu we have ( $f, \Delta\gamma_{BA}^0$  in  $\text{J m}^{-2}$ ) equal to  $(-0.007, > +1.40)$ ,  $(-0.018, +1.06)$  and  $(-0.025, +0.45)$ , respectively. In order to apply the criterion in Eq. (51), we need also to have values for the second and third terms. The third term is easily estimated using the data in Table I. To evaluate the third term we need to estimate  $\omega_0$ . On the basis of the relation<sup>9</sup>  $\mu_0 = C_0 W_0$  we may take  $\mu = CW$ , so that  $\omega_0 = C_0/C$  and  $\omega_0 = 1$  when  $C = C_0$ . For  $\omega_0 = 1$  it follows from Fig. 3 that  $r \approx 0.25$  and  $0.65$  for  $M = 3$  and  $10$ , respectively, and then from Fig. 5 that  $E^{\text{ML}}/E_0^{\text{ML}} \equiv 2(2M)^2 F^{\text{ML}} \approx 30$  and  $800$ , respectively. On using stiffness constants for Fe from Ref. 14 and formulas for Voigt averages from Ref. 15 we find  $\mu \approx 0.9 \times 10^{11} \text{ N m}^{-2}$  and  $\nu \approx 0.27$ . The third term in Eq. (51) may now

be calculated. The three terms in this equation accordingly yield (in  $\text{J m}^{-2}$ ) 1.40,  $-1.39$ , and  $0.002$ , respectively, for  $M = 3$  and  $1.40$ ,  $-0.46$ , and  $0.002$ , respectively, for  $M = 10$ . For values of  $\omega_0$  other than 1 the last term can at most be two times larger and thus still negligible. We may accordingly conclude that FM growth is unlikely in Fe/Cu(100), and that Co/Cu(100) with  $\Delta\gamma_{BA}^0 = 1.06 \text{ J m}^{-2}$  is probably a borderline case, whereas Ni/Cu(100) with  $\Delta\gamma_{BA}^0 = 0.45 \text{ J m}^{-2}$  may be a clear case of FM growth. Of course, since the third term is proportional to  $f^2$ , it would become significant at misfits of the order of 10%, about 200 times larger than for the 0.7% of Fe/Cu.

Similar considerations apply to bcc Fe and Cr on Ag and Au that have the orientation relationship  $(100)_B \parallel (100)_A$ , and  $[010]_B \parallel [011]_A$ . In spite of the small misfits of  $-0.008$  and  $-0.006$  for Fe on Ag and Au and of  $-0.002$  for Cr on Ag, and the negative contribution of the side faces, FM growth is not possible because of the large positive  $\Delta\gamma_{BA}^0$  values,  $2.26$ ,  $1.50$ , and  $1.32 \text{ J m}^{-2}$ , respectively. For Cr on Au, with  $f = -0.0002$  and  $\Delta\gamma_{BA}^0 \approx 0.50 \text{ J m}^{-2}$ , the situation is similar to that for Ni on Cu. The predictions of Eq. (51) with the values of Table I are in part in disagreement with recent experimental data which claim FM growth for fcc Fe (Refs. 16–18) and Co (Ref. 19) on Cu(100), for bcc Fe on Ag(100) (Ref. 20) and Au(100),<sup>21</sup> and for bcc Cr on Ag(100) (Ref. 22) and Au(100).<sup>23</sup> Most of these conclusions were based on the evolution of the magnitude of the derivative high-energy Auger electron signal of the film materials at energies  $E > 600 \text{ eV}$  with film thickness. The signals were found to increase in a piecewise-linear manner and the first slope change was attributed to the beginning of the second monolayer. While this technique for the determination of the growth mode is well established now, it has to be used with some caution. In particular, the high-energy Auger electron signals are rather insensitive to the fine details of the growth mode. For example, in the growth of Fe on Mo(110) the low-energy (47 eV) Fe and the 186-eV Mo signals show a clear slope change at 1 ML while no slope change is discernible at this coverage in the 704-eV Fe peak and only a smaller change after completion of 2 ML.<sup>24</sup> The slope changes

TABLE I. Interatomic distances  $d$  and specific free-surface energies  $\gamma$  of metals (Ref. 10) discussed in the text.

	bcc Cr	bcc Fe	fcc Fe	fcc Co	Ni	Cu	Ag	Au
$d$ (Å)	2.884	2.886	2.539	2.509	2.492	2.556	2.889	2.884
$\gamma$ ( $\text{J m}^{-2}$ )	2.056	2.939	2.939	2.790	2.364	1.934	1.302	1.626



after completion of a monolayer decrease with decreasing packing density of the layer, which usually is accompanied by a decrease of the interplanar distance. For example, in the growth of Cu on W(100) even the slope change of the 63-eV Cu Auger signal, after the first monolayer, is very small.<sup>25</sup>

Thus the claims that FM growth occurs for Fe on Cu, Ag, and Au(100) and Co on Cu(100) have to be viewed with some caution, in particular as there is also some evidence to the contrary. (i) In the growth of Fe on Ag(100) no high-resolution electron energy loss (RHEED) specular-beam intensity oscillations, which are typical for monolayer-by-monolayer growth, could be seen under the same experimental conditions which produced such oscillations in the growth of Fe on Fe(100).<sup>26</sup> For Fe on Cu(100) the non-FM-type growth has been demonstrated with several techniques including RHEED specular-beam intensity oscillations,<sup>27</sup> photoelectron forward scattering,<sup>28,29</sup> and CO titration.<sup>29</sup> Of course, differences in the deposition conditions could cause differences in the growth mode. If, for example, the surface temperature is so low that the condensing atoms cannot diffuse across the surface to form the 3D clusters expected on the basis of the equilibrium growth mode criterion, then monolayer-by-monolayer-like ("quasi-FM") growth may occur.<sup>10</sup> An indication in this direction is the observation that Fe does not grow in the FM mode on Au(100) at 150°C (Ref. 21) and that Cr on Au(100) forms at approximately 120°C, initially a substitutional alloy.<sup>30</sup> Taking all this evidence into account it appears safe to conclude that the experimental data—excluding some controversial interpretations—are in agreement with the theoretical predictions of Eqs. (49) and (51).

Even though uncertainties in the value of the parameters entering the relevant equations still exist, the theoretical considerations seem to support the experimentally based conclusion that FM growth occurs for the system Ni on Cu(100). Nevertheless we need to have further recourse to experiment which, in itself, is risky because of the danger of alloying. Some of the early studies reported FM growth, most of them VW growth.<sup>31</sup> More recent work, using surface science techniques, such as Auger electron spectroscopy or photoelectron forward scattering, indicate FM growth up to about six monolayers<sup>32,33</sup> in agreement with the foregoing considerations.

## VIII. CONCLUSIONS

The following conclusions are of interest.

(1) The acceptability regime of a double-layer island

encloses the acceptability regime of a ML island containing the same number of atoms.

(2) The first-order solution of the implicit acceptability relation (43) is almost indistinguishable from the exact solution.

(3) The acceptable misfit  $f_a$  increases with increasing bonding ( $\omega_0$ ) and decreases with increasing island size ( $N$ ) having a lower limit of  $1/4N$  at zero bonding. Conversely, the island "size"  $N$  that falls within acceptable limits, being proportional to  $f^{-1}$  for given  $\omega_0$ , can be quite large when  $f$  is small enough. Also, for a misfit  $f=0.05$  the acceptability criterion will never be violated for an island size  $N=2$ , but when  $N=7$ , it will be violated when  $\omega_0 \lesssim 0.3$ .

(4) The energy ratios  $E^{\text{DL}}/E^{\text{ML}}=r$  are very insensitive to misfit; the maximum discrepancy between  $r$  values for  $f=f_a$ , satisfying Eq. (43), and  $f=0.05$  (for both  $N=2$  and  $N=7$ ) is less than 3%.

(5) The ratio  $r$  is everywhere less than unity (as may be seen from Figs. 3 and 4) and approaches the value  $(N/M)^4$  as  $\omega_0$  goes to zero. This implies that the energy contributions of disregistry and strain invariably increase the total energy in relation (51) so that it may become positive if  $\Delta\gamma_{BA}^0$  were negative and hence favors 3D rather than 2D growth.

(6) It may be concluded from Fig. 5 that the energy  $E_1^{\text{DL}}$  of a DL, in which the ML's are constrained to undergo the same deformation, is less than that of the corresponding ML when the number of atoms is small. However, since  $E_1^{\text{DL}}$  will increase more rapidly with size it will ultimately exceed that of the ML.

(7) Application of the growth mode criterion to some film-substrate systems of current interest predicts non-FM growth for Fe on Cu, Ag, and Au, and Cr on Ag(100) surfaces, in contradiction to some experiments but in agreement with others. Theoretically Co on Cu is a borderline case and Ni on Cu a clear VW case, depending on the reliability of surface energy data. In systems with small  $f$  and  $\gamma_B - \gamma_A$ , the criterion does not allow reliable predictions at present because of the uncertainties in the parameters involved.

## ACKNOWLEDGMENTS

Much of this work was done while one of the authors (J.H.v.d.M.) was a guest at the Technical University of Clausthal. The authors acknowledge financial support from the Research Foundation of the South African Council for Scientific and Industrial Research and Sonderforschungsbereich (SFB) Göttingen, Clausthal.

\*Permanent address: Physikalisches Institut der Technischen Universität Clausthal, D-3392 Clausthal-Zellerfeld, Federal Republic of Germany.

<sup>1</sup>E. Bauer, *Z. Kristallogr.* **110**, 372 (1958); J. H. van der Merwe, in *Chemistry and Physics of Solid Surfaces V*, edited by R. Vanselow and R. Howe (Springer-Verlag, Berlin, 1984), Chap. 16; E. Bauer and J. H. van der Merwe, *Phys. Rev. B* **33**, 3657 (1986).

<sup>2</sup>S. Stoyanov and I. Markov, *Surf. Sci.* **116**, 313 (1982).

<sup>3</sup>F. C. Frank and J. H. van der Merwe, *Proc. R. Soc. London, Ser. A* **198**, 205 (1949).

<sup>4</sup>J. H. van der Merwe, *J. Appl. Phys.* **41**, 4725 (1970); in *Treatise of Materials Science and Technology*, edited by H. Herman (Academic, New York, 1973), Vol. 2, pp. 1–100; *Philos. Mag. A* **45**, 127 (1982).

<sup>5</sup>H. Gollisch (private communication).

- <sup>6</sup>H. Gollisch, *Surf. Sci.* **175**, 249 (1986).
- <sup>7</sup>J. H. van der Merwe and W. A. Jesser, *J. Appl. Phys.* **63**, 1509 (1988).
- <sup>8</sup>J. A. Snyman and J. H. van der Merwe, *Surf. Sci.* **45**, 619 (1974).
- <sup>9</sup>J. H. van der Merwe, *Phys. Rev. B* **37**, 2829 (1988).
- <sup>10</sup>L. Z. Mezey and J. Giber, *Jpn. J. Appl. Phys.* **21**, 1569 (1982).
- <sup>11</sup>R. Kern, G. LeLay, and J. J. Metois, in *Current Topics in Materials Science*, edited by E. Kaldis (North-Holland, Amsterdam, 1979), Vol. 3, p. 132.
- <sup>12</sup>J. Gerkema and A. R. Miedema, *Surf. Sci.* **124**, 351 (1983).
- <sup>13</sup>A. R. Miedema and F. J. A. den Broeder, *Z. Metallkd.* **70**, 14 (1979).
- <sup>14</sup>H. B. Huntington, in *Solid State Physics*, edited by F. Seitz and D. Turnbull (Academic, New York, 1958), Vol. 7, p. 214.
- <sup>15</sup>J. P. Hirth and J. Lothe, *Theory of Dislocations* (McGraw-Hill, New York, 1968), Chap. 13 and table on p. 762.
- <sup>16</sup>Y. C. Lee, H. Min, and P. A. Montano, *Surf. Sci.* **166**, 391 (1986).
- <sup>17</sup>M. F. Onellion, C. L. Fu, M. A. Thompson, J. L. Erskine, and A. J. Freeman, *Phys. Rev. B* **33**, 7322 (1986).
- <sup>18</sup>D. Pescia, G. Zampieri, M. Stampanoni, G. L. Bona, R. F. Willis, and F. Meier, *Phys. Rev. Lett.* **58**, 2126 (1987).
- <sup>19</sup>D. Pescia, G. Zampieri, M. Stampanoni, G. L. Bona, R. F. Willis, and F. Meier, *Phys. Rev. Lett.* **58**, 933 (1987).
- <sup>20</sup>G. C. Smith, G. A. Padmore, and C. Norris, *Surf. Sci.* **119**, L287 (1982).
- <sup>21</sup>R. Germar, W. Dur, D. Pescia, and W. Gudat, *Verh. Dtsch. Phys. Ges.* **4**, 56 (1988).
- <sup>22</sup>D. A. Newstead, C. Norris, C. Binns, and P. C. Stephenson, *J. Phys. C* **20**, 6245 (1987).
- <sup>23</sup>G. Zajac, S. D. Bader, and R. J. Friddle, *Phys. Rev. B* **31**, 4947 (1985).
- <sup>24</sup>M. Tikhov and E. Bauer (unpublished).
- <sup>25</sup>E. Bauer, H. Poppa, G. Todd, and F. Bonczek, *J. Appl. Phys.* **45**, 5164 (1974).
- <sup>26</sup>B. Heinrich, K. B. Urquhardt, A. S. Arrott, J. F. Cochran, K. Myrtle, and S. T. Purcell, *Phys. Rev. Lett.* **59**, 1756 (1987).
- <sup>27</sup>D. A. Steigerwald and W. F. Egelhoff, Jr., *Surf. Sci.* **192**, L887 (1987).
- <sup>28</sup>S. A. Chambers, T. J. Wagener, and J. H. Weaver, *Phys. Rev. B* **36**, 8992 (1987).
- <sup>29</sup>D. A. Steigerwald, I. Jacob, and W. F. Egelhoff, Jr., *Surf. Sci.* **202**, 472 (1988).
- <sup>30</sup>M. C. Hanf, C. Pirri, J. C. Peruchetti, D. Bolmont, and G. Gewinner, *Phys. Rev. B* **36**, 4487 (1987).
- <sup>31</sup>S. Nakahara and E. C. Felder, *Thin Solid Films* **91**, 111 (1982), and references therein.
- <sup>32</sup>W. F. Egelhoff, Jr., *Phys. Rev. Lett.* **59**, 559 (1987).
- <sup>33</sup>Q.-G. Zhu, Y. Yang, E. D. Williams, and R. L. Park, *Phys. Rev. Lett.* **59**, 835 (1987).